THE ASTROPHYSICAL JOURNAL, 424:189–199, 1994 March 20

SUBMILLIMETER CONTINUUM SURVEY OF THE GALACTIC CENTER

D. C. LIS AND J. E. CARLSTROM[1]
Division of Physics, Mathematics, and Astronomy, California Institute of Technology, Pasadena, CA 91125
Received 1993 July 23; accepted 1993 September 28

ABSTRACT

We have conducted a survey of the 800 μm continuum emission from an $\sim 1^\circ.5 \times 0^\circ.2$ area around the Galactic center with the objective to study the distribution of high-density material in the nuclear disk and to investigate the contribution of high-mass star formation to the luminosity and ionization of this region. Toward known high-mass star-forming regions, such as Sgr B2 and Sgr C, the large-scale distribution of the submillimeter continuum emission, which traces the temperature-weighted column density of dust, correlates well with the distribution of the radio continuum and far-infrared emission. However, in the Sgr A complex and the vicinity of the radio arc the correlation between the distribution of GMC cores traced by the dust emission and those of compact far-infrared sources and compact H II regions is poor. This may indicate that many of the dust cores detected in our survey are heated by the diffuse external radiation field rather than embedded young stars. In particular, there is no evidence for embedded far-infrared sources or compact H II regions associated with the dust cores located in a dust ridge which bridges the radio arc and Sgr B1. These dust cores may be unusually cold.

The two major sites of high-mass star formation in the nuclear disk, Sgr B2 and Sgr C, appear to coincide with the location of the inner Lindblad resonance. This region has been suggested as a location of enhanced star formation in circumnuclear regions of a number of barred galaxies.

Subject headings: Galaxy: center — ISM: clouds — ISM: individual (Sagittarius A, Sagittarius B, Sagittarius C) — stars: formation

1. INTRODUCTION

Molecular line emission surveys (e.g., Bania 1977; Liszt & Burton 1978; Heiligman 1987; Bally et al. 1987, 1988) have revealed a large concentration of dense molecular gas in the inner ~ 500 pc of the Milky Way. Giant Molecular Clouds (GMCs) in this region appear distinctly different from those in the Galactic disk (see Güsten 1989 for a review). They are characterized by high mean volume densities ($\sim 10^4$ cm^{-3}), gas temperatures (~ 60 K), and large internal velocity dispersions (~ 20–50 km s^{-1} FWHM). The bulk of the molecular gas is confined to a thin 30–50 pc layer often referred to as the nuclear disk. However, some clouds are displaced by several scale heights from the mean plane of symmetry and have velocities forbidden by Galactic rotation, indicating highly inclined, noncircular orbits.

The total far-infrared luminosity and the ionizing flux inferred from radio continuum observations of the Galactic center region imply a rate of star formation per unit mass of molecular material comparable to that in the Galactic disk (Mezger & Pauls 1979; Güsten 1989). However, H_2O and OH masers commonly found in sites of high-mass star formation are relatively rare in the nuclear disk (Güsten & Downes 1983). Boissé et al. (1981) and Odenwald & Fazio (1984) suggested that the formation rate of stars with masses greater than ~ 20 $M_\odot$ is decreased in the Galactic center compared to the disk. Cox & Laureijs (1989) suggested that the population of old cool stars in the bulge is the dominant heating source for the dust. Morris (1989) also argued that star formation could be currently suppressed in the Galactic center and that a substantial fraction of the far-infrared and radio continuum emission may be due to other processes.

The high gas pressures implied by observations of the diffuse X-ray emission suggest that GMCs in the nuclear disk may be held together by external pressure rather than self-gravity (Spergel & Blitz 1992). The gravitational collapse leading to the formation of high-density cores may thus be suppressed in all but the most massive clouds. The geometry and strength of magnetic fields may also play an important role in preventing gravitational collapse and formation of high-density cores at a rate comparable to that observed in the Galactic disk (Morris 1989). The importance of these dynamical effects for high-mass star formation can be most easily ascertained by studying the distribution of high-density material. This can be done through observations of *proper* molecular tracers. Due to the high mean volume density of the molecular gas (comparable to the critical density of the CS $J = 2 \rightarrow 1$ transition) the existing CO and CS surveys of the Galactic center (e.g., Bally et al. 1987; Heiligman 1987) show the distribution of the molecular material in the extended cloud envelopes. The high-energy transitions of high-dipole molecules, such as CS $J = 5 \rightarrow 4$, are good tracers of the molecular material in GMC cores. However, the lines are typically weak and make extensive surveys difficult. Submillimeter continuum emission, which traces the temperature-weighted column density of dust, has proven effective for determining column densities and masses of the emitting material in star-forming regions (e.g., Leung 1976; Westbrook et al. 1976; Keene, Hildebrand, & Whitcomb 1982; Mezger et al. 1986, 1989; Goldsmith, Snell, & Lis 1987; Gordon & Jewell 1987; Goldsmith et al. 1990). We have therefore conducted a survey of the 800 μm continuum emission from the nuclear disk to study the distribution of GMC cores in this region.

2. OBSERVATIONS

The data were taken on eight nights in 1992 May and July using a single-channel ^{3}He-cooled silicon bolometer mounted

[1] NSF Young Investigator.

in the Cassegrain focus of the 10.4 m Leighton telescope of the Caltech Submillimeter Observatory on Mauna Kea, Hawaii. A description of the CSO bolometer is given in Lis, Carlstrom, & Keene (1991). The data were taken under fair to moderate weather conditions characterized by a 225 GHz optical depth of ~0.07–0.11 at zenith. The noise equivalent flux density was ~5–6 Jy $Hz^{-0.5}$ at an air mass of 1.6. In spite of relatively high opacity, the atmospheric transmission was quite stable over the period of observations as indicated by a linear dependence of the logarithm of the observed flux density of Uranus and Sgr B2(N) as a function of air mass. The frequency response of the bolometer filter convolved with the atmospheric transmission curve and a power-law source with the ν^2 frequency dependence is shown in Figure 1. The mean frequency is ~380 GHz (~790 μm) and varies only slightly with the atmospheric transmission (by ~7 GHz for 225 GHz optical depths between 0.05 and 0.12).

To minimize the effect of the atmosphere, continuum observations are made in the beam switching mode. The bolometer output thus represents a flux difference between two positions on the sky, typically offset in azimuth. This observing mode results in spatial filtering of the extended emission on angular scales larger than the chopper throw used in the observations.[2] To recover the extended emission we employed the on-the-fly (OTF) fast mapping technique recently implemented at the CSO. The data were taken as the telescope was scanned across the source at a constant speed. The scans were taken at constant elevation and had a total length of ~12′–15′. The scanning rate was 10″ per second, and the data were sampled every 0.3 s (equal to the time constant of the lock-in amplifier; this results in a 3″ pixel size on the sky in the direction of the scan). The elevation spacing between the neighboring scans was 5″ or 10″.

[2] The chopper throw used during the present observations was ~180″–200″, and the chopping frequency was 10–12 Hz.

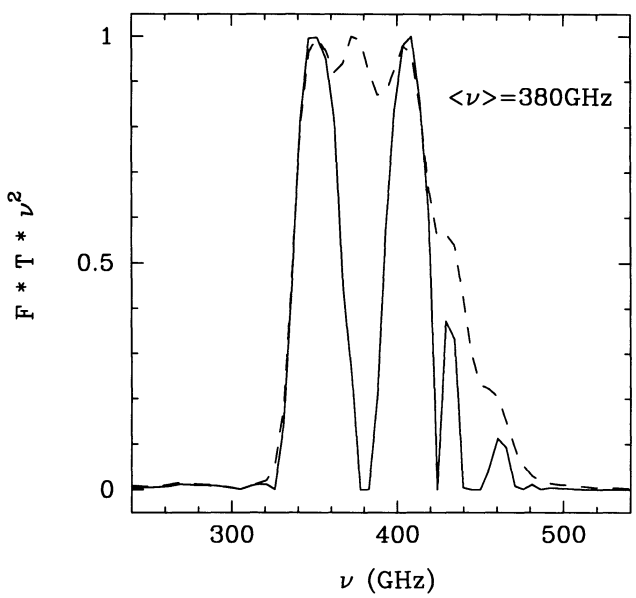

FIG. 1.—Frequency response of the 800 μm bolometer filter and the 20″ Winston cone used during the observations (*dashed line*) together with the frequency response convolved with the atmospheric transmission curve and a ν^2 source emission spectrum (*solid line*). The central dip in the convolved curve is caused by an atmospheric water vapor line. The mean frequency is 380 GHz (790 μm) and varies only slightly with the atmospheric opacity (by ~7 GHz for 225 GHz optical depths between 0.05 and 0.12).

Since the scan direction was the same as the chopper throw direction, the resulting differential images were reconstructed to the equivalent single beam images using the NOD 2 algorithm of Emerson, Klein, & Haslam (1979). The restored images were then interpolated onto a regular grid in the equatorial coordinate system. The total number of independent data points used for the final map is ~218,000 (equivalent to ~18 hours of integration). The focal plane aperture (defined by a Winston cone) was 20″, and the angular resolution of the interpolated image is ~30″ (FWHM).

The pointing accuracy of the telescope was checked directly from OTF maps of Sgr B2(N) and Uranus and was found to be stable over the period of observations. The appropriate corrections were applied to the data before they were transformed to the equatorial coordinate system. The absolute position uncertainties are $\lesssim$5″.

To remove the dependence of the observed signal on the air mass we made frequent maps of the Sgr B2(N) continuum source, the strongest compact source in the area. From the observed intensity as a function of air mass we derived average optical depths for each observing night which we used to scale the data to a reference air mass of 1.6. The average optical depths across the bolometer filter were ~0.5–0.9 at zenith. Since Sgr B2(N) was observed over the same air-mass range as other sources covered in the survey, a good relative calibration (~15%) was assured. The absolute flux calibration was done through OTF observations of Uranus. With a 3.″8 diameter and a 88 K brightness temperature (as determined from the fit to the measurements of Ulich, Dickel, & de Pater 1984; Hildebrand et al. 1985; and Orton et al. 1986), the flux density of Uranus at the time of observations was ~94 Jy at the reference frequency of 380 GHz. The corresponding flux densities of Sgr B2(N) and (M), the strongest compact sources in our map, are 342 and 307 Jy, respectively, in a 30″ beam. To verify our absolute calibration we compared these values with the submillimeter flux densities in the same beam measured by Goldsmith et al. (1990; 350–1100 μm) and Lis et al. (1991; 1300 μm). The 800 μm flux densities we measured agree to within $\lesssim$5% with the values obtained from the least-squares fit to the previous measurements.

3. MORPHOLOGY OF THE SUBMILLIMETER DUST EMISSION

A contour map of the 800 μm continuum emission from the nuclear disk is shown in Figure 2. The dotted line outlines the area covered in the CSO survey (~1.°5 × 0.°2). The integrated flux density within the region mapped is 13.6 kJy at the reference frequency of 380 GHz, corresponding to an H_2 mass of ~4×10^6 $M_\odot$.[3] One-half of the total integrated flux comes from regions with a flux density above 10.5 Jy in a 30″ beam. For a 30 K dust temperature this corresponds to an H_2 column density of 1×10^{23} cm^{-2}. There is a strong asymmetry in the intensity of the submillimeter continuum emission between the positive and negative Galactic longitudes. About one-half of the integrated 800 μm flux density comes from the Sgr B2

[3] In calculating H_2 masses and column densities we used the same grain parameters as adopted for Galactic center GMC cores by Lis et al. (1991), namely a grain radius of 0.1 μm, a mean grain density of 3 g cm^{-3}, a mean dust temperature of 30 K, and a H_2-to-dust ratio of 100 by mass (no correction for the cosmic helium abundance was applied). Interpolation of the 125 μm grain emissivity given by Hildebrand (1983; 7.5×10^{-4}) with a $\nu^{1.5}$ frequency dependence leads to a 800 μm emissivity of 4.7×10^{-5}. We adopted a 8.5 kpc distance to the Galactic center. The column density and mass estimates are functions of the mean dust temperature. They are ~80% higher if the dust temperature is 20 K and ~20% lower if the dust temperature is 40 K.

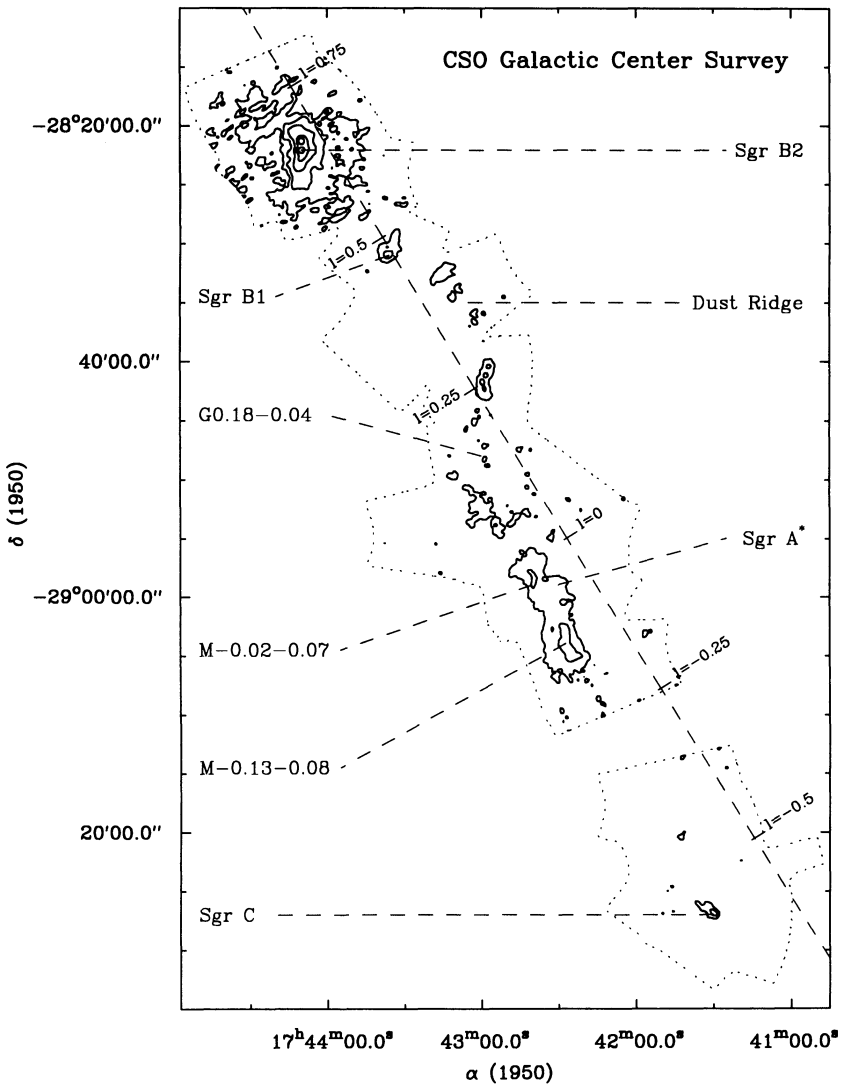

FIG. 2.—Contour map of the 800 μm continuum emission toward the nuclear disk. The angular resolution is 30″ FWHM. Contour levels are 8, 18, 40, 100, and 200 Jy. The peak intensity is 342 Jy toward Sgr B2(N). The area covered in the CSO survey is outlined by the dotted line. The location of the Galactic plane is marked with the dashed line. Notice the strong asymmetry between the positive and negative Galactic longitudes.

complex. The integrated flux density toward Sgr C is less than ~20% of that observed toward Sgr B2. A similar asymmetry is also seen in molecular data (e.g., Bally et al. 1987). In the following sections we discuss the morphology of the dust sources detected in our map.

3.1. *Sagittarius A Complex*

A contour map of the 800 μm continuum emission toward the Sgr A complex is shown in Figure 3. The distribution of the dust emission resembles that of the (1, 1) transition of ammonia (Güsten, Walmsley, & Pauls 1981; Okumura et al. 1989). The two peaks of the 800 μm emission correspond to the compact GMCs M−0.13−0.08 and M−0.02−0.07, often referred to as the "20 km s^{-1}" and "50 km s^{-1}" clouds (e.g., Güsten et al. 1981; Güsten 1989). Zylka, Mezger, & Wink (1990), based on their isotopic CO and CS data concluded that the Sgr A complex may consist of up to five distinct clouds which partially overlap in space and velocity.

The peak of the 800 μm emission in M−0.13−0.07 corresponds approximately to the stronger of the two compact 1300 μm sources detected by Zylka et al. (1990). The far-infrared survey of Odenwald & Fazio (1984) did not reveal any discrete far-infrared sources associated with this cloud (positions of compact far-infrared sources are marked by stars in Fig. 3). The extended far-infrared emission is also relatively weak. The cloud is seen in emission at 125 μm (Dent et al. 1982; however, no 55 μm emission is detected. Together with the weak C^+ emission (Genzel et al. 1989, 1990) this led Zylka et al. (1990) to the conclusion that M−0.18−0.08 is located ~50 pc away from the Galactic center, in front of the stellar cluster. The absence of compact far-infrared sources indicates that the external UV radiation is the dominant heating source for the dust. However, the 800 μm emission peak is located close to the radio continuum source G classified as a compact H II region by Ho et al. (1985). This, together with the presence of H_2O masers (Güsten & Downs 1983; Okumura et al. 1989), indicates that high-mass star formation is taking place in the core of this cloud.

Figure 3 shows two interesting filamentary features in M−0.13−0.08 (these are much more prominent in the false-

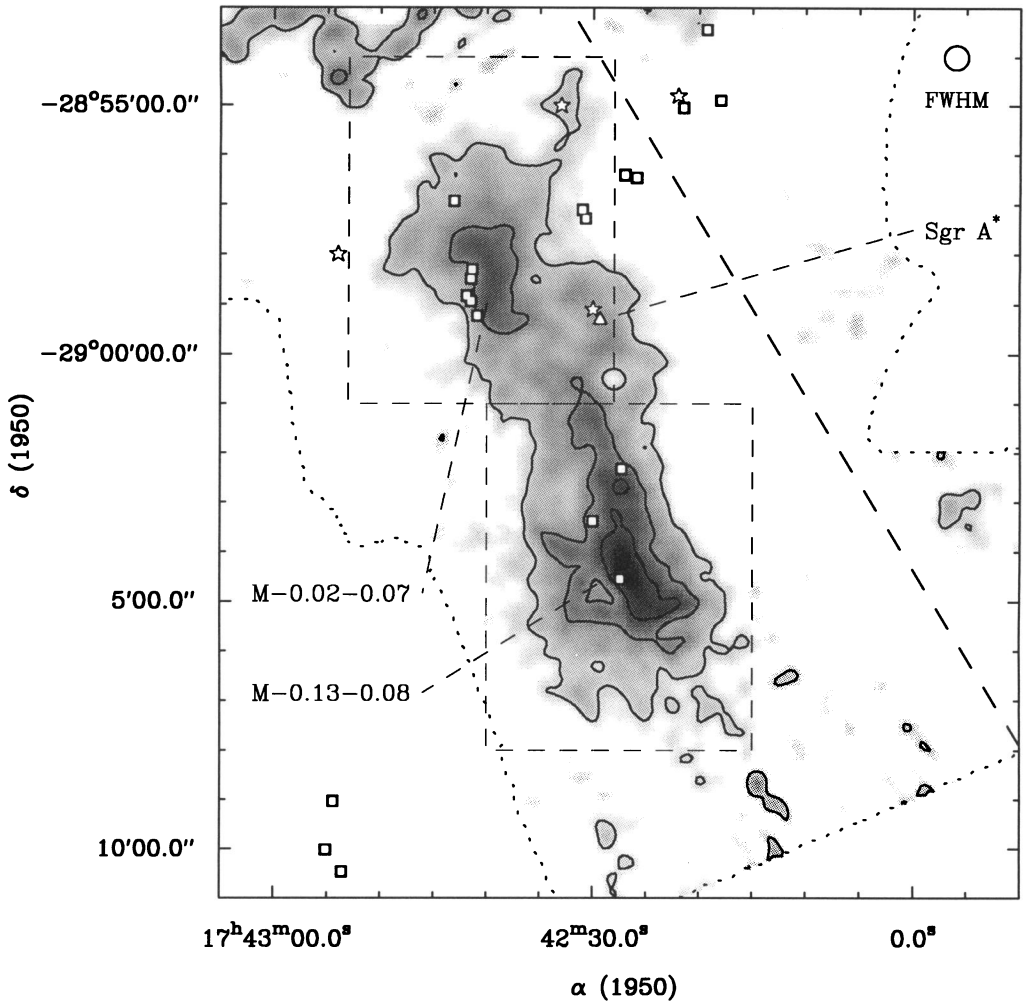

FIG. 3.—Contour map of the 800 μm continuum emission toward the Sgr A complex. Contour levels are 8, 16, 24, and 32 Jy in a 30″ FWHM beam. The two peaks of the emission correspond to the "20 km s^{-1}" and "50 km s^{-1}" clouds. Symbols mark the positions of compact far-infrared sources (*stars*; Odenwald & Fazio 1984), compact radio-continuum sources (*squares*; Yusef-Zadeh & Morris 1987), and Sgr A* (*triangle*). Notice the filamentary structures east of the 800 μm peak in the "20 km s^{-1}" cloud.

color representation of the map)—a closed loop of 800 μm emission, ~60″ (2.5 pc) in diameter, located southeast of the 800 μm peak, and a finger extending to the east of the peak. The second feature may be part of a shell surrounding the nonthermal radio continuum source E (Ho et al. 1985).

The secondary peak of the 800 μm emission in Figure 3 corresponds to M−0.02−0.07, a compact GMC adjacent to the nonthermal radio shell Sgr A East. The $C^{18}O$ $J = 2 \rightarrow 1$ (Genzel et al. 1990) and CS $J = 5 \rightarrow 4$ emission (Serabyn, Lacy, & Achtermann 1991) in this region peak along the eastern edge of Sgr A East indicating compression of the molecular cloud by the expanding radio shell source. The core of M−0.02−0.08 harbors a cluster of compact H II regions A–D (Ekers et al. 1983; Yusef-Zadeh & Morris 1987) and has been suggested as a region in which star formation has been induced by the interaction with the expanding radio source. However, Serabyn et al. (1991) argued that the compression wave has not yet reached the part of the cloud core which harbors the H II regions. The dust continuum emission peaks along the CS ridge—the H_2 column density observed toward the H II regions is relatively low. The good correlation between the distributions of the CS $J = 5 \rightarrow 4$ emission and the dust continuum suggests that both trace the H_2 column density. However, Figure 3 shows that the string of compact H II regions follows closely the eastern edge of the molecular cloud traced by the 800 μm emission. This spatial coincidence is puzzling if the compact H II regions were indeed produced in an earlier episode of star formation, unrelated to the interaction with Sgr A East.

The peak 800 μm flux densities toward M−0.13−0.08 and M−0.02−0.07 in a 30″ beam and the flux density integrated over the boxes outlined by the thin dashed line in Figure 3 are given in Table 1, together with the corresponding H_2 column densities and masses. Zylka et al. (1990) derived an H_2 mass of 2.7×10^5 $M_\odot$ for M−0.13−0.08 based on their 1300 μm continuum measurements. The difference between their mass estimate and ours may be considered a measure of the uncertainties in the column density and mass estimates due to the poorly known grain parameters and the mean dust temperature. Molecular mass estimates of M−0.02−0.07 based on the $C^{18}O$ $J = 2 \rightarrow 1$ and CS $J = 5 \rightarrow 4$ data are 2×10^5 (Genzel et al. 1990) and 1.5×10^5 $M_\odot$ (Serabyn et al. 1991), respectively.

3.2. *Radio Continuum Arc*

The radio arc is one of the most prominent features in radio continuum maps of the Galactic center region (e.g., Althenhoff et al. 1978). It consists of a number of thermal and nonthermal

TABLE 1

PARAMETERS OF THE DUST SOURCES

Source	α (1950)	δ (1950)	S_p	S_t	θ[a]	N_{H_2}	M
Sgr B2	$17^h44^m09^s.9$	−28°21′20″	342	6710	800 × 600	3.8×10^{24}	2×10^6
Sgr B1	17 43 36.4	−28 31 00	27	210	180 × 120	3.0×10^{23}	8×10^4
Dust ridge[b]	17 42 59.8	−28 41 40	24	1490	900 × 120	2.6×10^{23}	5×10^5
M−0.02−0.07	17 42 00.0	−28 59 00	22	990	340 × 180	2.4×10^{23}	4×10^5
M−0.13−0.08	17 42 27.0	−20 04 20	37	1280	420 × 200	4.1×10^{23}	5×10^5
Sgr C	17 41 29.8	−29 26 54	26	1230	160 × 60	1.1×10^{23}	5×10^5

NOTES.—Entries in the table are source, position of the 800 μm emission peak, peak flux density in a 30″ beam (Jy), integrated flux density (Jy), approximate source size (arcseconds), peak H_2 column density (cm^{-2}), and the cloud mass ($M_\odot$). The column densities and masses are calculated using the dust temperature of 30 K, with the exception of Sgr C where a temperature of 67 K was used to calculate the peak H_2 density (Lis et al. 1991).

[a] An approximate source size within an 8 Jy contour which corresponds to an H_2 column density of $\sim 1 \times 10^{23}$ cm^{-2}.

[b] Excluding Sgr B1.

components. The nonthermal part of the arc is made of narrow linear filaments which intersect the Galactic plane at an approximately right angle at a Galactic longitude of ∼0°.18 (Yusef-Zadeh, Morris & Chance 1984). These filaments are considered to be the manifestation of highly organized poloidal magnetic field present throughout the inner 50 pc of the Galaxy (Morris & Yusef-Zadeh 1989). The thermal part of the arc, often referred to as the "bridge," is a system of arched filaments which connect at a right angle to the northern end of the nonthermal filaments and gradually bend toward the plane (Morris & Yusef-Zadeh 1989). A weaker system of thermal arched filaments is also seen on the opposite side of the Galactic plane.

A contour map of the 800 μm continuum emission toward

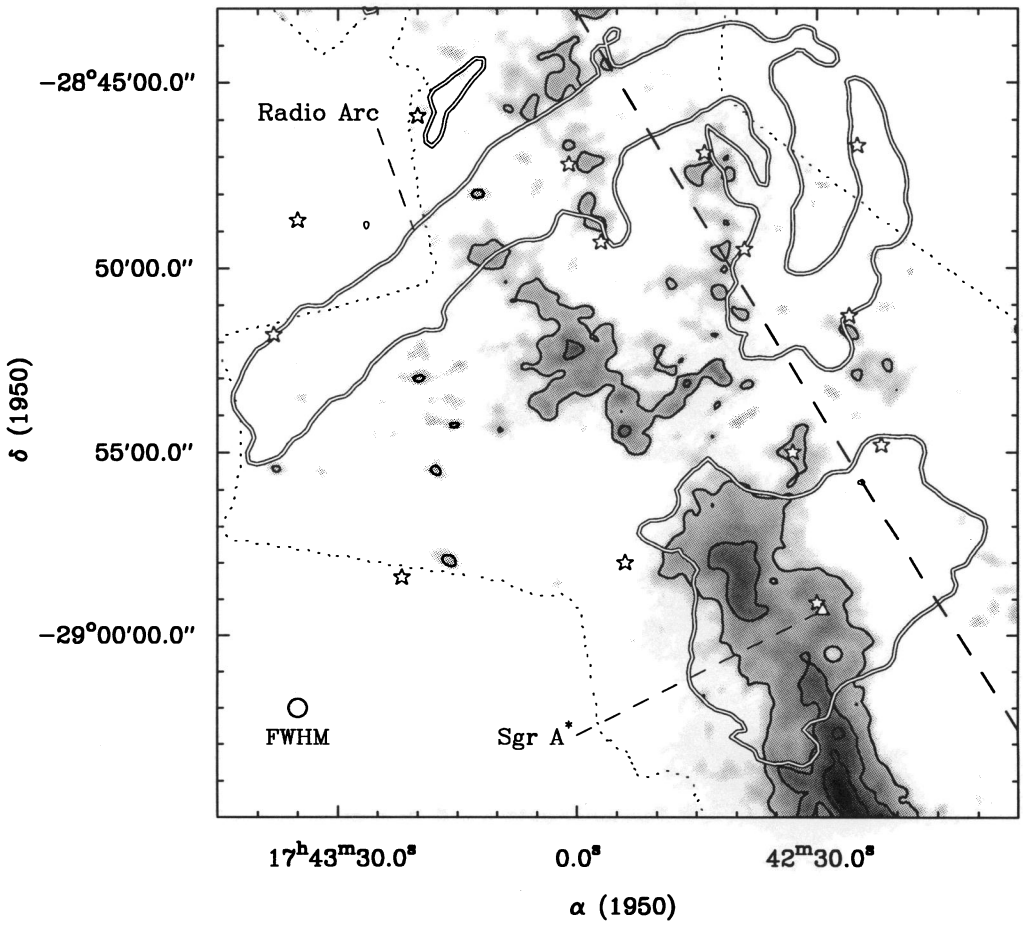

FIG. 4.—Contour map of the 800 μm continuum emission toward the Galactic center arc. Contour levels are 8, 16, 24, and 32 Jy in a 30″ FWHM beam. The submillimeter map shows three ridges of emission approximately perpendicular to the nonthermal filaments. The western ridge is adjacent to, but does not overlap with, the thermal arched filaments. The northern ridge intersects the nonthermal filaments at the location of the radio continuum source G0.18−0.04. The eastern ridge appears a continuation of the "50 km s^{-1}" cloud, although there is a depression of the continuum emission at the intersection with the thermal arched filaments. Stars mark the positions of compact far-infrared sources (Odenwald & Fazio 1984). Double contours outline the region of 20 cm emission (Yusef-Zadeh 1986). Notice the apparent lack of correlation between the distribution of the dust emission and that of the radio continuum emission.

the arc region is shown in Figure 4 together with an outline of the 20 cm radio continuum emission (Yusef-Zadeh 1986). The distribution of the 800 μm emission is similar to that of the (1, 1) ammonia emission (Güsten et al. 1981). The 800 μm map shows three ridges of emission in the vicinity of the arc each of them approximately perpendicular to the nonthermal filaments. There is little overlap between the dust emission and the radio continuum emission in the vicinity of the thermal arched filaments. The 800 μm emission terminates near the thermal filament E1 (Morris & Yusef-Zadeh 1989)—no emission is observed to the west, toward the filaments E2, W1, and W2. This is consistent with the conclusion of Serabyn & Güsten (1987) that the arched filaments lie primarily along edges of molecular clouds traced by the CS emission. The CS emission appears somewhat more spatially extended than the dust continuum. However, the CS $J = 2 \rightarrow 1$ integrated intensity in the -55 to 5 km s^{-1} velocity range shows essentially the same components as those seen in our 800 μm map, namely the emission toward the western dust ridge, around the radio continuum sources H3–H7 (Yusef-Zadeh & Morris 1987), and near the end of the southern dust ridge pointing toward Sgr A. Morris & Yusef-Zadeh (1989) suggested Alfvén's critical ionization velocity effect (Alfvén 1954) as a possible source of ionization in this region. However, photoionization by recently formed OB stars cannot be ruled out (Genzel et al. 1990). No 800 μm emission is seen near the southern group of thermal filaments.

The northern dust ridge intersects the nonthermal part of the arc near the location of the radio continuum source G0.18 $-$ 0.04. Yusef-Zadeh & Morris (1987) suggested that this is a region of strong collisional ionization at the intersection of thermal and nonthermal filaments. The dust continuum delineates the ambient neutral cloud threaded by the magnetic field lines, which was previously observed in the CS $J = 3 \rightarrow 2$ emission by Serabyn & Güsten (1991). Yusef-Zadeh & Morris (1987) suggested the relativistic particles associated with the nonthermal filaments as a probable source of ionization in this region. However, Serabyn & Güsten (1991) argued in favour of the Alfvén's critical ionization velocity effect. There are two compact far-infrared sources associated with this region (FIR 12 and 33; Odenwald & Fazio 1984). However, no compact H II regions have been found (Yusef-Zadeh & Morris 1987). It is thus unclear whether star formation is taking place there.

3.3. *Sagittarius B2*

Sagittarius B2 has been studied extensively in molecular emission by Lis & Goldsmith (1989, 1990, 1991) and in the submillimeter and millimeter continuum by Goldsmith et al. (1987, 1990). The distribution of the 800 μm emission is shown in Figure 5 and the fluxes, column density, and mass are given

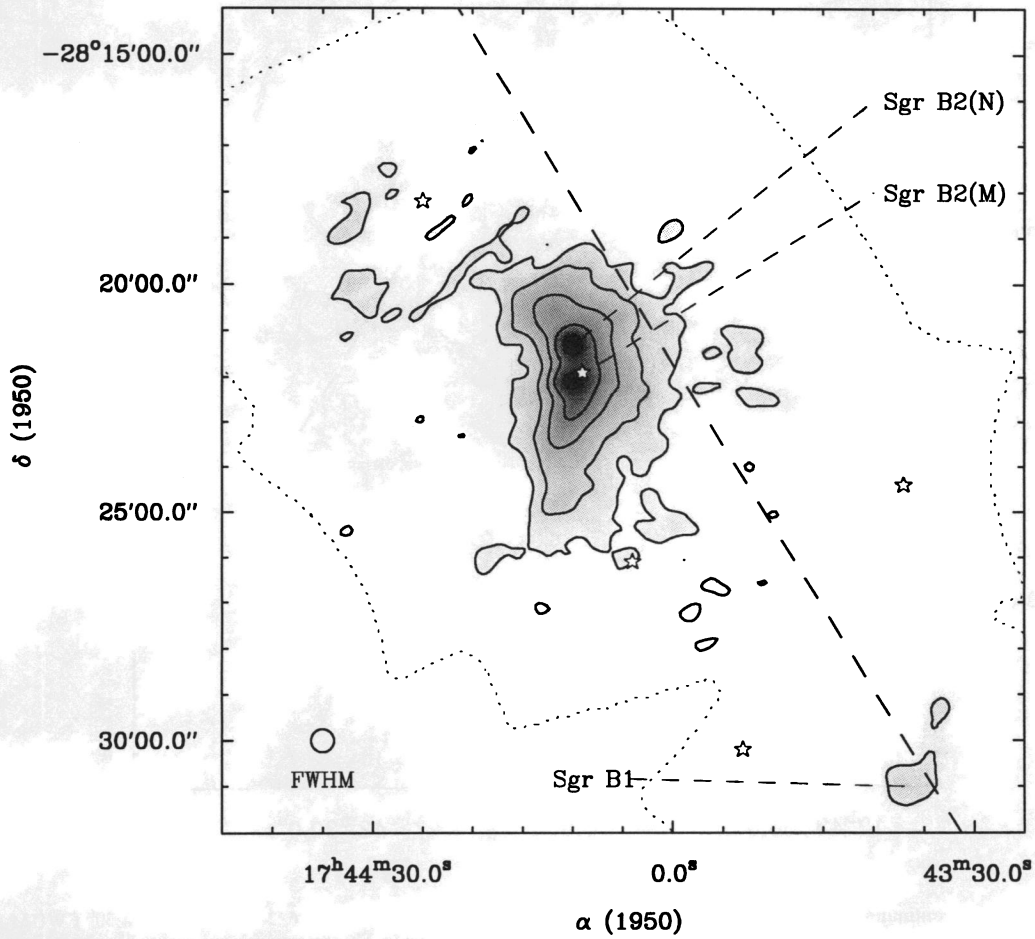

FIG. 5.—Contour map of the 800 μm continuum emission toward the Sgr B complex. Contour levels are 15, 30, 60, 120, and 250 Jy in a 30″ FWHM beam. The two peaks correspond to the Sgr B2(N) and (M) continuum sources. Sgr B1 is located in the lower-right corner of the map. Stars mark the positions of compact far-infrared sources (Odenwald & Fazio 1984).

in Table 1. As discussed above, the peak 800 μm flux densities toward the Sgr B2(N) and (M) continuum source agree to within 5% with previous submillimeter measurements. The mass we derive here is a factor of 3 higher than previous estimates based on dust continuum emission ($\sim 8 \times 10^5\ M_\odot$; Lis et al. 1991; Gordon et al. 1993). Our mass estimate is only a factor of 3 lower than the mass of the extended molecular cloud derived by Lis & Goldsmith (1989) based on their isotropic CO observations ($6 \times 10^6\ M_\odot$). This indicates that we have detected a significant fraction of the emission from the extended cloud. However, due to the large angular extent of the Sgr B2 envelope, a portion of the extended emission may still be filtered out in our data.

Figure 5 shows relatively strong 800 μm emission ($\sim$75 Jy) $\sim 1'$ northeast of Sgr B2(N) where strong $HOCO^+$ and HNCO emission is observed (Minh, Irvine, & Ziurys 1988; Lis & Goldsmith 1990). Both these molecules are considered probes of the infrared radiation field. Interestingly, no far-infrared sources are detected in this region. Since our data have been taken with a broad-band filter, the relatively strong emission in this region may be caused by increased molecular line contamination. The remaining compact far-infrared sources detected in the Sgr B2 area by Odenwald & Fazio (1984; marked as stars in Fig. 5) do not appear to have associated compact dust cores.

The southernmost far-infrared source in Figure 5 is associated with the H II region Sagittarius B1. A strong compact dust source (peak 800 μm flux density of 27 Jy in a 30″ beam) is found $\sim 4'$ west of the far-infrared source and the H II region. There appears to be no compact H II regions or far-infrared sources associated with the dust core. However, Mehringer, Palmer, & Goss (1993) reported a tentative detection of an H_2O maser coinciding with the dust core, which is located near the boundary of the area they surveyed.

3.4. *Sagittarius C*

Sagittarius C can be considered a counterpart of Sgr B2, being situated at a similar distance from the Galactic center but at negative Galactic longitude. It is a strong source of radio continuum emission (Kapitzky & Dent 1974; Downes et al. 1978). Far-infrared emission observations of Gatley et al. (1977) show emission peaking at a wavelength shorter than 100 μm, suggesting an optical depth much lower than in Sgr B2. The far-infrared luminosity and Lyman continuum flux are consistent with those of a single O4 ZAMS star (Odenwald & Fazio 1984).

The distribution of the 800 μm emission in the Sgr C complex is shown in Figure 6. The observed flux densities and H_2 column density and mass estimates are given in Table 1. The low-level 800 μm emission to the east and northwest of the peak correspond to maxima of the CS $J = 2 \rightarrow 1$ and ^{13}CO

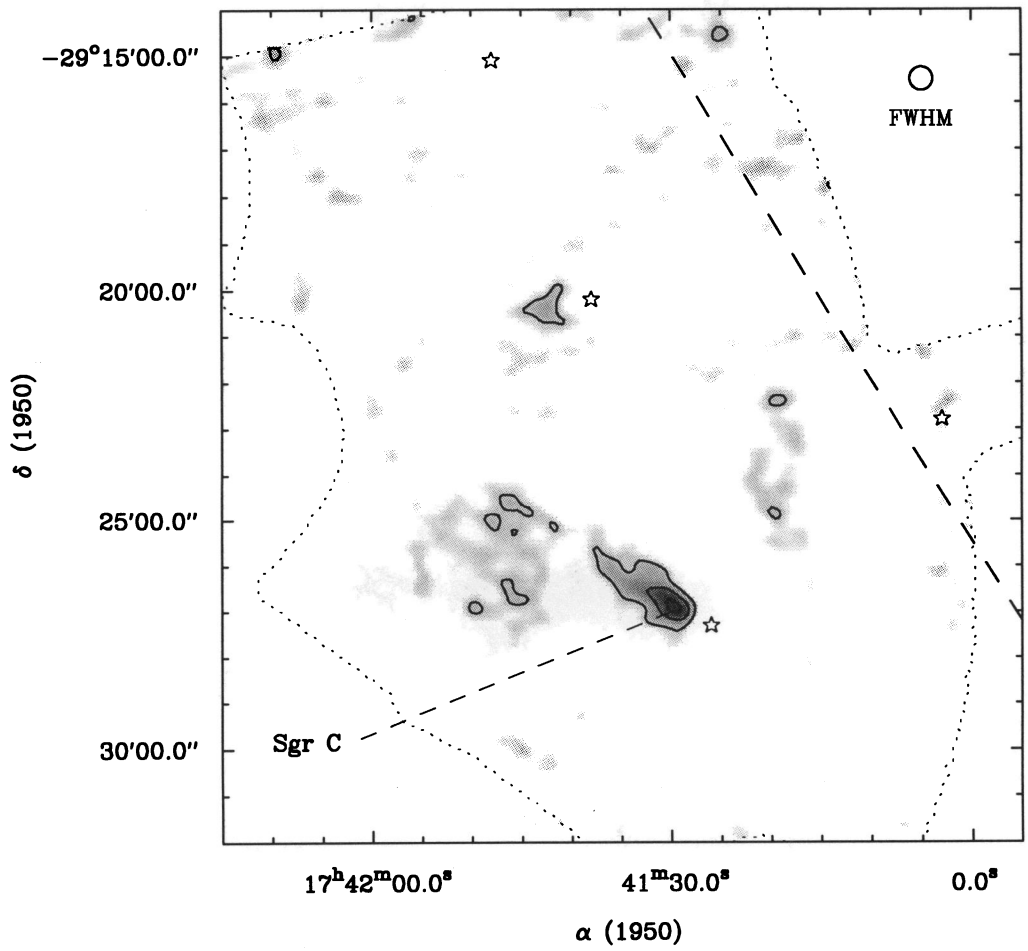

FIG. 6.—Contour map of the 800 μm continuum emission toward Sgr C. Contour levels are 8, 16, and 24 Jy in a 30″ FWHM beam. Stars mark the positions of compact far-infrared sources (Odenwald & Fazio 1984).

$J = 1 \rightarrow 0$ integrated intensity in the -55 and -100 km s^{-1} clouds, respectively (Lis et al. 1994). The dust core itself is located close to the edge of the -55 km s^{-1} component. The 800 μm emission peak $\sim 7'$ north of Sgr C is associated with the far-infrared source FIR 5 (Odenwald & Fazio 1984) located in a separate GMC with a mean LSR velocity of -35 km s^{-1} (Lis et al. 1994).

3.5. *Dust Ridge*

One of the most interesting features in the 800 μm dust continuum map shown in Figure 2 is the narrow, clumpy ridge of emission apparently connecting Sgr B1 and the radio continuum source G0.18 $-$ 0.04 associated with the Galactic center radio arc. An expanded view of this feature is shown in Figure 7. The strong 800 μm peak north of G0.18 $-$ 0.04, just outside of the nonthermal part of the arc, corresponds to the ammonia peak M0.25 + 0.01 (Güsten et al. 1981). No compact radio continuum sources (Downes et al. 1978) or compact far-infrared sources (Odenwald & Fazio 1984) are seen toward the dust cores in the ridge. We have started a search for compact H II regions and H_2O masers in this region to determine whether star formation is taking place in the dust cores.

Limited CS $J = 5 \rightarrow 4$ data taken along the ridge at the CSO indicate gas velocities between 0 and 40 km s^{-1}. Channel maps of low angular resolution (100″) CS $J = 2 \rightarrow 1$ data in this velocity range (Bally et al. 1987) show a morphology similar to that of the dust emission. The velocity of the gas in this ridge is also similar to that of the molecular cloud associated with the radio continuum source G0.18 $-$ 0.04 (Serabyn & Güsten 1991). This suggests that the ridge may be physically connected to the arc. If the ridge represents a coherent kinematic structure, it must have formed quite recently as it would be dispersed by the differential rotation on the timescale of a few times 10^6 yr (but see § 6).

4. ORIGIN OF THE SUBMILLIMETER EMISSION

Schmidt (1978) separated the thermal and nonthermal radio continuum emission from the Galactic center region. He estimated the integrated flux density in the thermal component to be ~ 950 Jy at 5 GHz. For optically thin free-free emission ($S_\nu \sim \nu^{-0.1}$) the corresponding 800 μm flux density is ~ 600 Jy. The free-free emission thus contributes only $< 5\%$ of the integrated 800 μm flux density (the contribution could be higher if a significant fraction of the 5 GHz flux comes from optically thick components).

Broad-band continuum emission may be contaminated strongly by molecular lines. Sutton et al. (1984) estimated that $\sim 40\%$–60% of the broad-band 1300 μm flux density in Orion A may be due to line emission. However, the corresponding

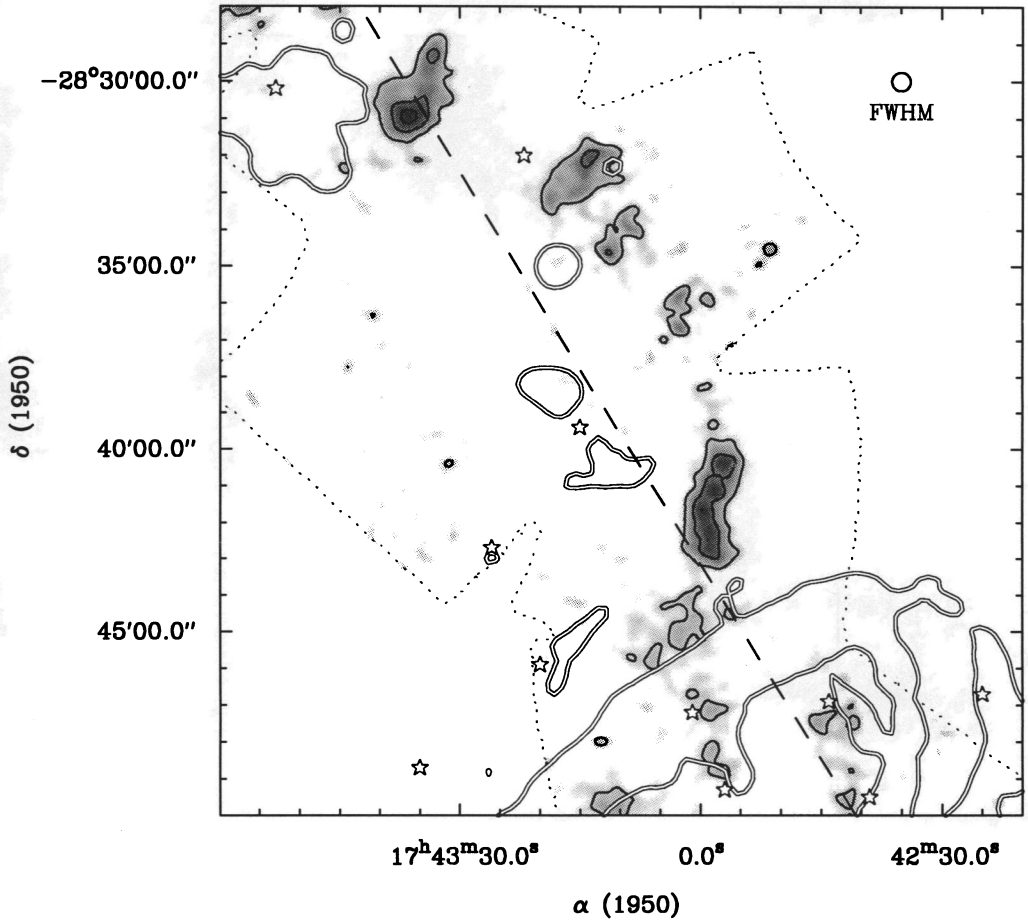

FIG. 7.—Contour map of the 800 μm continuum emission toward the dust ridge. Contour levels are 8, 16, and 24 Jy in a 30″ FWHM beam. Limited CS $J = 5 \rightarrow 4$ data suggest a coherent structure which connects to the Galactic center radio arc. Stars mark the positions of compact far-infrared sources (Odenwald & Fazio 1984). Double contours outline the region of 20 cm emission (Yusef-Zadeh 1986). Notice the apparent lack of correlation between the distribution of the dust emission with that of the radio continuum emission and with compact far-infrared sources.

value for Orion 1:5 S is only ~15%. It is thus unclear whether the strong line contribution inferred for Orion A is representative of GMC cores. Lis & Goldsmith (1991) suggested that ~30% of the broad-band flux density near 355 GHz in a 20″ beam toward the *compact cores* in Sgr B2 is likely to come from molecular lines. The line contamination is likely to be lower in less active Galactic center sources. Throughout this paper we thus assumed that the submillimeter continuum emission is produced exclusively by dust at a temperature of ~30 K. Our column densities and masses may be overestimated for sources with significant line contamination. However, conclusions concerning the *general morphology* of the dense gas are not affected, as both the dust continuum and line emission tend to be strongest toward GMC cores.

Although our survey covers the most extended region mapped in submillimeter continuum at high angular resolution, it is still plausible that significant fraction of the extended continuum emission (on scales larger than the 12′–15′ scan length) may be filtered out in our map. To estimate the magnitude of the spatial filtering we compared our integrated 800 μm flux density with the 300 μm flux density from the low-resolution survey of the Galactic plane by Hauser et al. (1984). Figure 4 of Hauser et al. gives a mean brightness of $\sim 2 \times 10^9$ Jy sr^{-1} over the region $l = \pm 0.^\circ 75$, $b = \pm 0.^\circ 5$, corresponding to a total 300 μm flux density of ~900 kJy within this region which leads to a total 800 μm flux density of ~30 kJy, assuming a $\nu^{3.5}$ frequency dependence as determined from the integrated flux densities in Sgr B2 (Goldsmith et al. 1990). An upper limit for the 800 μm flux density *within the region we mapped* can be obtained assuming that all the flux measured by Hauser et al. comes from this region. Under this assumption we recover ~45% of the large beam flux. A more realistic estimate of the total 800 μm flux within the area covered by our survey can be made assuming a Gaussian distribution for the 300 μm emission in Galactic latitude with a given scale height. Hauser et al. give a scale height of ~0.°9 (FWHM) based on their far-infrared and submillimeter data. This is a factor of ~3–4 larger than the scale height of the molecular gas layer (~0.°25 or 40 pc). If we assume that the 300 μm continuum emission observed by Hauser et al. has a scale height of 0.°25, we estimate that ~60% of the 300 μm flux comes from the region covered in our survey. This implies a total 800 μm flux density of ~18 kJy within the region we mapped and indicates that ~75% of the total 800 μm flux is detected in our map. One should keep in mind, however, that there are significant uncertainties involved in the two flux measurements as well as in the interpolation between the 300 and 800 μm wavelengths; the above estimate is not very well constrained.

Unless there is a strong molecular line contamination, the submillimeter continuum traces temperature-weighted column density of dust. The emission maxima correspond to regions with the highest H_2 column densities (GMC cores). The elevated dust temperatures in the vicinity of newly formed stars make the continuum observations particularly well suited for studies of high-mass star-forming regions. However, strong dust continuum is also observed toward sources which show no direct evidence for the presence of embedded young stellar objects and are presumably cold, but with very high column density (e.g., NGC 2024; Mezger et al. 1988).

5. STAR FORMATION IN THE GALACTIC CENTER

Odenwald & Fazio (1984) measured an integrated far-infrared flux density of 1.7×10^6 Jy at an effective wavelength of 70 μm. The far-infrared emission comes primarily from a presumably optically thin extended component, ~3° × 0.°5 in size. Only ~15% of the FIR luminosity comes from discrete sources. If the dust responsible for the far-infrared emission has a mean temperature of 70 K (Odenwald & Fazio 1984) and a $\nu^{1.5}$ emissivity law between 70 and 800 μm, it contributes a flux density of ~1.8 kJy at 800 μm, a small fraction (~13%) of the observed flux. This calculation shows that the far-infrared and submillimeter emission trace different dust components, a conclusion further supported by the difference in the spatial distributions of the two tracers. With the exception of a few known star-forming regions, like Sgr B2 and Sgr C, most of the dust cores detected in our survey show no evidence for the presence of associated far-infrared sources. This is true in particular for the compact sources in the dust ridge and indicates that the dust is heated by the external radiation field rather than by embedded young stars.

The small number of discrete far-infrared sources detected in their survey led Odenwald & Fazio (1984) to the conclusion that formation of stars earlier than O7.5 is currently suppressed at the Galactic center. They noted that the observed luminosity and ionization of the Galactic center region can be explained by a population of 300,000 stars with spectral types between B0 and B3. Alternatively, the apparent absence of stars earlier than O7.5 in the Galactic center could be explained if the high-mass star formation suddenly stopped there some 2×10^6 years ago (the main-sequence lifetime of an O7.5 star). Odenwald & Fazio argue that this scenario is rather unlikely as it would have resulted in ~160,000 stellar remnants produced over such a period of time, in apparent contrast to the small number of known supernova remnants found in the region. However, model calculations of Shull (1980) and Wheeler, Mazurek, & Sivramakrishnan (1980) suggest that supernova remnants embedded in dense gas may not be observable as nonthermal radio sources and may only be detectable in the infrared. Brouillet & Schilke (1993) suggested that this process may be responsible for the apparent anticorrelation between the distribution of supernova remnants and dense molecular clumps in M82. If this were the case for the Galactic center one would then expect, in contrast with the observations, a good correlation of the location of IR sources and the 800 μm dust emission.

An alternative explanation for the observed deficiency of O-type stars in the Galactic center region, favored by Odenwald & Fazio (1984), is a modified IMF with a low formation frequency for stars more massive than ~20 $M_\odot$. Even in this scenario, however, it is unclear whether the less massive B-type stars, presumably responsible for the observed extended far-infrared luminosity and ionization of the Galactic center region, *currently* form there at a rate comparable to that in the Galactic disk. As discussed above, many GMC cores detected in our survey do not show evidence for the presence of internal heating sources. It is thus plausible that the star formation is currently suppressed in the nuclear disk even for stars less massive than 20 $M_\odot$.

Morris (1993) suggested that the low end of the IMF in the inner 10 pc region may also differ from the Salpeter IMF. He argued that stars form in this region as a result of compression of their parent molecular clouds rather than the process of gravitational collapse. This mechanism would favor formation of more massive stars compared to the Galactic disk and would increase the lower cutoff for the IMF maybe up to ~1 $M_\odot$. At present there is no quantitative calculations to support this idea. However, it is possible that the population of stars

that formed (or are currently forming) in the Galactic center region may be confined to a rather narrow mass range of ~ 1–$20\ M_\odot$.

The physical process leading to the formation of GMC cores may be a clue to the small number of early-type stars detected in the Galactic center region. Dust emission traces the column density and, in principle, does not discriminate between the low and high volume density regions. However, in the regions mapped in the $J = 5 \rightarrow 4$ transition of CS dust emission has been found to correlate well with the CS emission (e.g., Lis et al. 1994). This indicates that sources bright in the submillimeter continuum are most likely dense. The relatively small number of strong dust sources we detect suggests that deficiency of early-type stars may be related to the small fraction of gas at high volume densities. For example, in the case of Sgr C the material with the H_2 column density greater than 10^{23} cm^{-2} which is bright in the dust continuum and CS $J = 5 \rightarrow 4$ emission (and is therefore dense) contains only a small fraction of the total molecular mass (Lis et al. 1994). The formation of GMC cores in the Galactic center may be suppressed by disruptive tidal forces (e.g., Güsten 1989), strong magnetic fields (Morris 1989), or high gas pressures (Spergel & Blitz 1992). Detailed studies of the dust cores detected in our survey will be important for understanding the processes leading to the cloud collapse and high-mass star formation in the Galactic center.

6. DYNAMICAL RESONANCES IN THE NUCLEAR DISK

Galactic bars cause strong density enhancements and, especially when resonances exist, a substantial increase in the collisional rate of molecular clouds. Devereux (1987) and Dressel (1988) showed that the highest incidence of starbursts occur in barred S0–Sa galaxies. Kenney et al. (1992) showed that the strongest CO emission in three barred galaxies arises from *twin peaks*, which are oriented perpendicular to the large-scale stellar bars and located where dust lanes intersect nuclear ring of H II regions. These twin gas concentrations can be explained by the crowding of gas streamlines near inner Lindblad resonances. In a recent paper Telesco, Dressel, & Wolstencroft (1993) studied the location of starburst regions (as traced by mid-infrared continuum emission) in 21 galaxies, most of which were barred or showed evidence for oval distortions. They concluded that the most intense star formation occurs near the inner Lindblad resonances (ILRs) when ILRs exist or at the nuclei when ILRs do not exist. This may suggest that GMCs tend to form at the ILRs by coalescence resulting from enhanced collision rates. Alternatively, the high collision rates may lead to enhanced star formation by compression of the gas at cloud interfaces.

There is increasing evidence that the potential in the center of our own Galaxy is nonaxisymmetric. The existence of a bar in the Milky Way was first suggested by de Vaucouleurs (1964) based on the comparison of the amplitude of noncircular motions with those observed in external barred galaxies. Binney et al. (1991) presented a coherent dynamical model of the H I, CO, and CS from the inner 10° region of the Galaxy. They concluded that the flow of the gas at the Galactic center is dominated by a bar that has a corotation at ~ 2.4 kpc, which we view at an inclination angle of $\sim 16°$ from its major axis. In their model, the molecular ring at ~ 3.5 kpc is probably associated with the outer Lindblad resonance of the bar. Direct photometric evidence for the presence of the bar based on the distribution of the 2.4 μm continuum emission was presented by Blitz & Spergel (1991).

The two most prominent high-mass star-forming regions in the nuclear disk, Sgr B2 and Sgr C, are located at projected galactocentric distances of ~ 100 and 75 pc, respectively. The location of the inner Lindblad resonance is given by the condition $\kappa = 2(\Omega - \Omega_b)$, where κ is the epicyclic frequency (the frequency of the radial oscillations in the reference frame comoving with the bar), $\Omega = V(r)/r$ is the angular velocity, and Ω_b is the angular resolution of the bar. If $\Omega_b = 81$ km s^{-1}, as suggested by Binney et al. (1991), and the rotation curve in the inner 800 pc is that given by Burton & Gordon (1978), the inner Lindblad resonance is located at the galactocentric radius of ~ 110 pc. It is thus plausible that the Sgr B2 and C complexes are closely associated with the inner Lindblad resonance.

The origin of the dust cores in the ridge between Sgr B1 and the radio arc may also be related to the nonaxisymmetric mass distribution in the vicinity of the Galactic center. The small velocity shifts between different positions along the ridge might be easily explained if the dust cores correspond to density enhancement along the leading edge of the bar. In this scenario one would expect a symmetric structure on the opposite side of the Galactic center, at negative longitudes. Such a structure does not appear to be present. However, the region at negative Galactic longitudes has not been properly sampled in our survey (there is a gap in the sky coverage between Sgr A and Sgr C in Fig. 2). Moreover, the emission from the counterpart of the dust ridge between the radio arc and Sgr B1 may be substantially weaker as a result of the overall asymmetry in the distribution of gas between the positive and negative Galactic longitudes.

7. CONCLUSION

We carried out a survey of the 800 μm continuum emission from $\sim 1.5 \times 0.^\circ 2$ area around the Galactic center. The 800 μm emission, which traces temperature-weighted column density of dust, reveals the location of GMC cores in the nuclear disk. With the exception of a few known high-mass star-forming regions, like Sgr B2 and Sgr C, the distribution of the dust emission is poorly correlated with those of the far-infrared and radio continuum emission. This suggests that many of the dust cores detected in our survey may be heated by the external radiation field rather than embedded young stars. In particular, at present there is no evidence for high-mass star formation in taking place in the compact dust cores in the dust ridge above the radio arc.

The bar suggested by dynamical models of Binney et al. (1991) and independently confirmed photometrically by Blitz & Spergel (1991) may play an important role in explaining the location of two major sites of high-mass star formation in the nuclear disk, Sgr B2 and Sgr C. It appears that these two complexes may be closely related to the location of the inner Lindblad resonance. The region near the inner Lindblad resonance has been suggested by Telesco et al. (1993) as a preferred place for high-mass star formation in the circumnuclear regions of a number of barred galaxies. The bar may also be responsible for the dust ridge which bridges the radio arc and Sgr B1.

We thank K. Young for implementing and debugging the continuum on-the-fly mapping mode at the CSO, M. Morris for the 20 cm continuum image of the Galactic center, as well as a number of stimulating discussions, and P. Goldsmith for his comments concerning this manuscript. This research has been supported by NSF grant AST 90-15755 to the Caltech Submillimeter Observatory.

REFERENCES

Alfvén, H. 1954, On the Origin of the Solar System (Oxford: Oxford Univ. Press)
Althenhoff, W. J., Downes, D., Pauls, T., & Schraml, J. 1978, A&AS, 35, 23
Bally, J., Stark, A. A., Wilson, R. W., & Henkel, C. 1987, ApJS, 65, 13
———. 1988, ApJ, 324, 223
Bania, T. M. 1977, ApJ, 216, 381
Binney, J., Gerhard, O. E., Stark, A. A., Bally, J., & Uchida, K. I. 1991, MNRAS, 252, 210
Blitz, L., & Spergel, D. N. 1991, ApJ, 379, 631
Boissé, P., Gispert, A., Coron, N., Wijnberger, J. J., Serra, G., Ryter, C., & Puget, J. L. 1981, A&A, 94, 265
Brouillet, N., & Schilke, P. 1993, A&A, 277, 381
Burton, W. B., & Gordon, M. A. 1978, A&A, 63, 7
Cox, P., & Laureijs, R. 1989, in The Center of the Galaxy, ed. M. Morris (Dordrecht: Kluwer), 121
Dent, W. A., Werner, M. W., Gatley, I., Becklin, E. E., Hildebrand, R. H., Keene, J., & Whitcomb, S. E. 1982, in The Galactic Center, ed. R. Riegler & R. Blandford (AIP Conf. Proc. 83), 33
de Vaucouleurs, G. 1964, in IAU Symp. 20, The Galaxy and the Magellanic Clouds, ed. F. Kerr & A. Rodgers (Sydney: Australian Academy of Science), 195
Devereux, N. 1987, ApJ, 323, 91
Downes, D., Goss, W. M., Schwartz, U. J., & Wouterloot, J. G. A. 1978, A&AS, 35, 1
Dressel, L. L. 1988, ApJ, 329, L69
Ekers, R. D., Van Gorkom, J. H., Schwarz, U. J., & Goss, W. M. 1983, A&A, 122, 143
Emerson, D. T., Klein, U., & Haslam, C. G. T. 1979, A&A, 76, 92
Gatley, I., Becklin, E. E., Werner, M. W., & Wynn-Williams, C. G. 1977, ApJ, 216, 277
Genzel, R., Stacey, G. J., Harris, A. I., Townes, C. H., & Geiss, N. 1989, in The Center of the Galaxy, ed. M. Morris (Dordrecht: Kluwer), 151
Genzel, R., Stacey, G. J., Harris, A. I., Townes, C. H., Geis, N., Graf, U. U., Poglitsch, A., & Stutzki, J. 1990, ApJ, 356, 160
Goldsmith, P. F., Lis, D. C., Hills, R., & Lasenby, J. 1990, ApJ, 350, 186
Goldsmith, P. F., Snell R. L., & Lis, D. C. 1987, ApJ, 313, L5
Gordon, M. A., Berkermann, U., Mezger, P. G., Zylka, R., Haslam, G., Kreysa, E., & Sievers, A. 1993, A&A, in press
Gordon, M. A., & Jewell, P. R. 1987, ApJ, 323, 766
Güsten, R. 1989, in The Center of the Galaxy, ed. M. Morris (Dordrecht: Kluwer), 89
Güsten, R., & Downs, D. 1983, A&A, 117, 343
Güsten, R., Walmsley, C. M., & Pauls, T. 1981, A&A, 103, 197
Hauser, M. G., Silverberg, R. F., Stier, M. T., Kelsall, T., Gezari, D. Y., Dwek, E., Walser, D., & Mather, J. C. 1984, ApJ, 285, 74
Heiligman, G. M. 1987, ApJ, 314, 747
Hildebrand, R. H. 1983, QJRAS, 24, 267
Hildebrand, R. H., Loewenstei, R. F., Harper, D. A., Orton, G. S., Keene, J., & Whitcomb, S. E. 1985, Icarus, 64, 64
Ho, P. T. P., Jackson, J. M., Barrett, A. H., & Armstrong, J. T. 1985, ApJ, 288, 575
Kapitzky, J. E., & Dent, W. A. 1974, ApJ, 188, 27
Keene, J., Hildebrand, R. H., & Whitcomb, S. E. 1982, ApJ, 252, L11
Kenney, J. D. P., Wilson, C. D., Scoville, N. Z., Devereux, N. A., & Young, J. S. 1992, ApJ, 395, L79
Leung, C. M. 1976, ApJ, 209, 75
Lis, D. C., Carlstrom, J. E., & Keene, J. 1991, ApJ, 380, 429
Lis, D. C., & Goldsmith, P. F. 1989, ApJ, 337, 704
———. 1990, ApJ, 356, 195
———. 1991, ApJ, 369, 157
Lis, D. C., Goldsmith, P. F., Carlstrom, J. E., & Bergin, E. A. 1994, in preparation
Liszt, H. S., & Burton, W. B. 1978, ApJ, 226, 790
Mehringer, D. M., Palmer, P., & Goss, W. M. 1993, ApJ, 402, L69
Mezger, P. G., Chini, R., Kreysa, E., & Gemünd, H.-P. 1986, A&A, 160, 324
Mezger, P. G., Chini, R., Kreysa, E., Wink, J. E., & Salter, C. J. 1988, A&A, 191, 44
Mezger, P. G., & Pauls, T. 1979, in The Large-Scale Characteristic of the Galaxy, ed. W. Burton (Boston: Reidel), 357
Mezger, P. G., Zylka, R., Salter, C. J., Wink, J. E., Chini, R., Kreysa, E., & Tuffs, R. 1989, A&A, 209, 337
Minh, Y., Irvine, W. M., & Ziurys, L. 1988, ApJ, 334, 175
Morris, M. 1989, in The Center of the Galaxy, ed. M. Morris (Dordrecht: Kluwer), 171
———. 1993, ApJ, 408, 496
Morris, M., & Yusef-Zadeh, F. 1989, ApJ, 343, 703
Odenwald, S. F., & Fazio, G. G. 1984, ApJ, 283, 601
Okumura, S. K., et al. 1989, ApJ, 347, 240
Orton, G. S., Griffin, M. J., Ade, P. A. R., Nolt, I. G., Rodostitz, J. V., Robson, E. I., & Gear, W. K. 1986, Icarus, 67, 289
Schmidt, J. 1978, Ph.D. thesis, Univ. of Bonn
Serabyn, E., & Güsten, R. 1987, A&A, 184, 133
———. 1991, A&A, 242, 376
Serabyn, E., Lacy, J. H., & Achtermann, J. M. 1991, ApJ, 395, 166
Shull, M. J. 1980, ApJ, 37, 769
Spergel, D. N., & Blitz, L. 1992, Nature, 357, 665
Sutton, E. C., Blake, G. A., Masson, C. R., & Phillips, T. G. 1984, ApJ, 283, L41
Telesco, C. M., Dressel, L. L., & Wolstencroft, R. D. 1993, ApJ, 414, 120
Ulich, B. L., Dickel, J. R., & de Pater, I. 1984, Icarus, 60, 590
Westbrook, W. E., et al. 1976, ApJ, 209, 94
Wheeler, J. C., Mazurek, T. J., & Sivramakrishnan, A. 1980, ApJ, 37, 781
Yusef-Zadeh, F. 1986, in The Center of the Galaxy, ed. M. Morris (Dordrecht: Kluwer), 243
Yusef-Zadeh, F., & Morris, M. 1987, ApJ, 320, 545
Yusef-Zadeh, F., Morris, M., & Chance, D. 1984, Nature, 310, 557
Zylka, R., Mezger, P. G., & Wink, J. E. 1990, A&A, 234, 133